Molecular Biology of the Cell
Vol. 12, 3161–3174, October 2001

γ-Tubulin and the C-Terminal Motor Domain Kinesin-like Protein, KLPA, Function in the Establishment of Spindle Bipolarity in *Aspergillus nidulans*

Natalie L. Prigozhina*†, Richard A. Walker,‡ C. Elizabeth Oakley,* and Berl R. Oakley*§

*Department of Molecular Genetics, Ohio State University, Columbus, Ohio 43210; and ‡Department of Biology, Virginia Polytechnic Institute and State University, Blacksburg, Virginia 24061

Submitted May 10, 2001; Revised July 27, 2001; Accepted July 31, 2001
Monitoring Editor: Lawrence S. Goldstein

Previous research has found that a γ-tubulin mutation in *Schizosaccharomyces pombe* is synthetically lethal with a deletion of the C-terminal motor domain kinesin-like protein gene *pkl1*, but the lethality of the double mutant prevents a phenotypic analysis of the synthetic interaction. We have investigated interactions between *klpA*1, a deletion of an *Aspergillus nidulans* homolog of *pkl1*, and mutations in the *mipA*, γ-tubulin gene. We find that *klpA*1 dramatically increases the cold sensitivity and slightly reduces the growth rate at all temperatures, of three *mipA* alleles. In synchronized cells we find that *klpA*1 causes a substantial but transient inhibition of the establishment of spindle bipolarity. At a restrictive temperature, *mipA*D123 causes a slight, transient inhibition of spindle bipolarity and a more significant inhibition of anaphase A. In the *mipA*D123/*klpA*1 strain, formation of bipolar spindles is more strongly inhibited than in the *klpA*1 single mutant and many spindles apparently never become bipolar. These results indicate, surprisingly, that γ-tubulin and the *klp*A kinesin have overlapping roles in the establishment of spindle bipolarity. We propose a model to account for these data.

INTRODUCTION

The essential role of γ-tubulin in microtubule nucleation is now well established (reviewed by Wiese and Zheng, 1999; Oakley, 2000). Recent data from *Schizosaccharomyces pombe*, however, indicate that γ-tubulin has at least one additional essential but as yet incompletely defined function (Paluh *et al.*, 2000). One of the key findings that led to this conclusion was the fact that a mutant γ-tubulin allele was found to be synthetically lethal with a deletion of the C-terminal motor domain kinesin-like protein Pkl1p. This finding was surprising and clearly worthy of further study. The lethality of the double mutant, however, precluded any analysis of the synthetic effects of the two mutations on mitosis or the microtubule cytoskeleton. It is also of interest to determine whether interactions between mutant γ-tubulin alleles and deletions of C-terminal motor domains occur in organisms other than *S. pombe*.

Pkl1p (encoded by the *pkl1* gene) is a member of a family of proteins that play important but incompletely defined roles in mitosis and meiosis. This family includes, but is not limited to, KLPA (encoded by the *klpA* gene) of *Aspergillus nidulans*, Kar3p (encoded by the *KAR3* gene) of *Saccharomyces cerevisiae*, and Ncd (encoded by the *ncd* gene) of *Drosophila melanogaster*. Deletions of the *klpA*, *KAR3*, and *pkl1* genes are not lethal, but overexpression of these genes causes mitotic spindles to be very small and dysfunctional (O'Connell *et al.*, 1993; Pidoux *et al.*, 1996; Saunders *et al.*, 1997b). In meiosis I in oocytes, Ncd appears to function in spindle assembly and stabilization of the spindle in metaphase arrest (Matthies *et al.*, 1996, and earlier references therein).

Mutant alleles of this family exhibit important genetic interactions with mutations in genes that encode kinesins involved in mitotic spindle elongation. A temperature-sensitive allele of the *bimC* gene (*bimC*4) of *A. nidulans* inhibits spindle pole body (SPB) separation at restrictive temperatures (Enos and Morris, 1990) and deletion of *klpA* partially suppresses the temperature sensitivity of *bimC*4 (O'Connell *et al.*, 1993). Likewise, deletion or mutation of *KAR3* partially suppresses the spindle collapse caused by mutation or deletion of the spindle elongation motors Cin8p and Kip1p in *S. cerevisiae* (Roof *et al.*, 1992; Saunders and Hoyt, 1992; Hoyt

† Present address: The Scripps Research Institute, Department of Cell Biology, MB-39, Room MBB201, 10550 North Torrey Pines Rd., La Jolla, CA 92037.
§ Corresponding author. E-mail address: oakley.2@osu.edu.
Abbreviations used: DAPI, 4′,6-diamidino-2-phenylindole; MBP, maltose binding protein; SMI, spindle mitotic index; SPB, spindle pole body.

et al., 1993). These data have led to the suggestion that motors such as BIMC, Cin8p, and Kip1p bridge interpolar microtubules from opposite poles and push the poles apart. KLPA, Kar3p, Ncd, and Pkl1p have been suggested to provide an opposing force that pulls poles toward each other in mitosis (Saunders and Hoyt, 1992; O'Connell *et al.*, 1993; Pidoux *et al.*, 1996, reviewed by Sharp *et al.*, 2000).

Kar3p and Ncd are minus-end–directed motors (Walker *et al.*, 1990; Endow *et al.*, 1994) and a Kar3p fusion protein causes disassembly of taxol-stabilized microtubules in vitro, particularly at the minus end (Endow *et al.*, 1994). A deletion of the *KAR3* gene causes cytoplasmic microtubules to be abnormally long and abundant and these abnormalities can be mostly corrected by the antimicrotubule agents benomyl and nocodazole (Saunders *et al.*, 1997a). These data, in combination, have led to the suggestion that microtubule depolymerization might be the mechanism by which Kar3p opposes anaphase B motors and pulls spindle poles toward each other (Saunders *et al.*, 1997a).

Other data, however, seem to contradict the notion that this family of proteins in general, and Kar3p in particular, pulls mitotic spindle poles toward each other or, at least, suggest that the protein may have additional mitotic functions. Meluh and Rose (1990) found that >30% of KAR3 mutant cells in unsynchronized material had short spindles, whereas <1% had a similar phenotype in wild-type cells. The loss of a protein that pulls spindle poles together should, if that were its sole function, promote spindle elongation. The patterns of suppression of *Cin8/KIP1* double mutants by *KAR3* missense alleles also suggested that Kar3p might have some functions that overlap with Cin8p and Kip1p, perhaps in cross-bridging spindle interzone microtubules (Hoyt *et al.*, 1993). Cottingham *et al.* (1999) found that a *KAR3* mutation reduced the frequency of cells with bipolar spindles by 10–25% and that deletion of *KIP3* reduced the frequency of cells with bipolar spindles by 20–35%. These results suggest a role for *KAR3* in establishing bipolar spindles.

Data on the *SLK9* gene of *S. cerevisiae* are also germane to our understanding of KAR3p function. A functional *SLK19* gene was found to be required for viability in a *KAR3* deletion strain (Zeng *et al.*, 1999). Although a deletion of *SLK19* is not lethal, it does cause an increase in mitotic cells with a short, bipolar spindle and abnormally abundant cytoplasmic microtubules (Zeng *et al.*, 1999). When a strain carrying a deletion of *SLK19* and a temperature-sensitive *KAR3* allele was incubated at a restrictive temperature, it was arrested at G_2/M with a monopolar microtubule array (Zeng *et al.*, 1999). When the same strain was shifted from a permissive to a restrictive temperature, bipolar spindles collapsed and spindle poles moved toward each other, but if the spindles had entered anaphase by the time of the temperature shift, they persisted (Zeng *et al.*, 1999). Kar3p localizes to the SPB (Saunders *et al.*, 1997a; Zeng *et al.*, 1999), but Slk19p localizes mainly to centromeres and the spindle midzone (Zeng *et al.*, 1999). These data suggest that Kar3p and Slk19p have overlapping spindle stabilization functions and they seem, superficially, to be incompatible with the notion that Kar3p pulls spindle poles together. Indeed, if Kar3p pulls spindle poles together, reducing or eliminating Kar3p activity should, if anything, inhibit spindle collapse. The extent of the contradictions in the field is highlighted by the fact that reliable data from excellent labs have led to the diametrically opposite conclusions that Kar3p functions by promoting microtubule disassembly (Saunders *et al.*, 1997a) and that it functions by stabilizing microtubules (Zeng *et al.*, 1999).

We have recently completed an alanine scanning mutagenesis of the *A. nidulans* γ-tubulin (*mipA*) gene (Jung *et al.*, 2001). We now report that three conditionally lethal alleles, created by alanine scanning mutagenesis, exhibit strong synthetic interactions with *klpA*1, a deletion of the *klpA* gene. This indicates that interactions between γ-tubulin alleles and mutations in C-terminal motor domain kinesin-like proteins are probably general and are certainly not confined to *S. pombe.* We have examined the effects of a mutant *mipA* allele (*mipAD123), klpA*1 and the combination of *mipA*D123 and *klpA*1 on progression through mitosis. We have also expressed a KLPA fusion protein in *Escherichia coli* and examined its motor and microtubule bundling activities. In combination, our data suggest a model for KLPA and γ-tubulin function that may help to resolve some of the apparent contradictions in the field.

MATERIALS AND METHODS

A. nidulans Strains and Media

The strains used are listed in Table 1. Nim911, LO718, LO721, and LO782 were used for microscopic analyses. Media were YG (5 g/l yeast extract, 20 g/l D-glucose), YAG (YG with 15 g/l agar), or FYG (YG with 25 g/l pretested burtonite 44c (TIC Gums, Belcamp, MD). Because *pyr4* does not fully complement *pyrG*89 at low temperatures, we routinely supplemented these media with 10 mM uridine and 1 mg/ml uracil. For NIM911 and its progeny we supplemented with 50 μg/ml adenine, 0.02 μg/ml biotin, 300 μg/ml ammonium sulfate, 50 μg/ml methionine, 2 μg/ml niacin, and 20 μg/ml choline. For strains carrying *argB*2, we supplemented with 0.5 mg/ml arginine

*KlpA*1 is a replacement of the *klpA* gene with the *pyr4* gene of *Neurospora crassa* (O'Connell *et al.*, 1993). *KlpA*1 was followed through crosses by polymerase chain reaction (PCR) of genomic DNA with primers specific for *klpA* and for *pyr4*. Strains carrying *klpA*1 thus showed no amplification with the *klpA*-specific primers but did show amplification with the *pyr4*-specific primers. We verified that the restricted growth in the *mipA*D123/*klpA*1 double mutant was due to a synthetic interaction between *klpA*1 and *mipA*D123 (rather than some unlikely, but theoretically possible interaction with a background mutation), as follows (our unpublished data). We transformed the double mutant with plasmid pKK12-29, which carries a wild-type *klpA* cDNA under the control of the regulatable *alcA* promoter (O'Connell *et al.*, 1993). We then incubated transformants at a range of temperatures on media that repress expression from the *alcA* promoter, induce expression at moderate levels, or induce expression at high levels. On repressing media (i.e., little or no KLPA) the transformants were tightly cold sensitive like the *mipA*D123/*klpA*1 parent. On media that induced moderate levels of expression of KLPA, growth of the transformants was weakly cold sensitive like strains carrying *mipA*D123 and the wild-type allele of *klpA* (*klpA*+). On media that induced at high levels (i.e., KLPA overexpressed) growth was inhibited at all temperatures as has been observed previously (O'Connell *et al.*, 1993).

Growth of Cells for Microscopy

To ensure good cell adhesion, prewashed glass coverslips were covered with poly-L-lysine (Sigma, St. Louis, MO) according to the manufacturer's instructions. They were then sterilized by autoclaving. Synchronization of cells carrying *nimT*23 was accomplished as

Table 1. List of the *A. nidulans* strains used in this study. Note: strains listed as "progeny" may have additional nutritional markers

Strain	Strain description	Source
NIM911	*chaA*1, *nimT*23, *adE*20, *biA*1, *wA*2, *cnxE*16, *sC*12, *methG*1, *nicA*2, *lacA*1, *choA*1	N.R. Morris
FGSC154	*chaA*1, *adE*20, *biA*1, *wA*2, *cnxE*16, *sC*12, *methG*1, *nicA*2, *lacA*1, *choA*1	Fungal Genetics Stock Center
MO61	*argB*2, *nicA*2, *pabaA*1, *klpA*1 (*pyrG*$^+$, *pyr4*$^+$)	N.R. Morris
R153	*wA*3, *pyroA*4	C.F. Roberts
SO26	*nimT*23, *pyrG*89, *biA*1, *pabaA*1, *cnxE*16, *wA*2	S.A. Osmani
*mipA*D123	*mipA*D123, *pyrG*89, *fwA*1, *pabaA*1, *uaY*9	Jung *et al.*, 2001
LO701 = *mipA*D123/*klpA*1 (progeny of *mipA*D123 and MO61)	*mipA*D123, *klpA*1, *pabaA*1 (*pyrG*$^+$, *argB*$^+$, *pyr4*$^+$)	This study
LO721 = *mipA*D123/*nimT*23 (progeny of LO701 and SO26)	*mipA*D123, *nimT*23, *pabaA*1 (*pyrG*$^+$)	This study
LO718 = *mipA*D123/*klpA*1/*nimT*23 (progeny of LO701 and SO26)	*mipA*D123, *klpA*1, *nimT*23, *wA*2, *cnxE*16, *pabaA*1	This study
LO782 = *klpA*1/*nimT*23 (progeny of LO701 and SO26)	*klpA*1, *nimT*23, *pabaA*1 (*pyrG*$^+$, *sC*$^+$)	This study
LO694 (progeny of *mipA*D123 and FGSC154)	*mipA*D123, *sC*12, *pabaA*1, *wA*2 (*pyrG*$^+$, *adE*$^+$, *biA*$^+$, *metG*$^+$, *nicA*$^+$, *cnxE*$^+$, *choA*$^+$)	This study
LO776 = *mipA*H370 (progeny of LO771 and FGSC 442)	*mipA*H370, *chaA*1, (*pyrG*+)	This study
LO771	*mipA*H370, *pyrG*89, *fwA*1, *pabaA*1, *uaY*9	Jung *et al.*, 2001
FGSC442	*facB*101, *riboB*2, *chaA*1, *sE*15, *nirA*14	Fungal Genetics Stock Center
LO807 = *mipA*H370/*klpA*1 (progeny of LO771 and MO61)	*mipA*H370, *fwA*1, *klpA*1 (*pyrG*+, *argB*+)	This study
LO699	*mipA*D159, *pyrG*89, *fwA*1, *pabaA*1, *uaY*9	Jung *et al.*, 2001
LO635 = *mipA*D159	*mipA*D159, *pabaA*1, *fwA*1	This study
LO705 = *mipA*D159/*klpA*1 (progeny of LO699 and MO61)	*mipA*D159, *klpA*1, *argB*2 (*pyrG*+)	This study

follows. Sterile coverslips were placed in Petri dishes and covered by liquid medium. Conidia were inoculated into the medium and the Petri dishes were placed in styrofoam floats in a 43°C water bath (with holes cut out so the bottoms of the dishes were in direct contact with water). They were incubated at this temperature for 8–8.5 h during which time they settled onto and adhered tightly to the coverslips. They were shifted from 43 to 20°C by rapidly aspirating the warm medium, replacing it with medium precooled to 20°C, and placing the Petri dishes in an incubator at 20°C.

Preparation of Cells for Immunofluorescence Microscopy

Fixation and all washes were carried out in miniature Coplin jars, and cell wall digestion was performed by placing the coverslips germling side down onto 250-μl drops of the appropriate solution on parafilm. Cells were fixed by placing coverslips in miniature Coplin jars containing fixative at the same temperature as the culture medium. The fixative was prepared fresh by mixing equal volumes of 16% formaldehyde (Electron Microscopy Sciences, Fort Washington, PA) and fixation buffer, consisting of 100 mM piperazine-*N*,*N*′-bis(2-ethanesulfonic acid) (PIPES) (Roche Molecular Biochemicals, Indianapolis, IN), pH 6.7, 50 mM EGTA (Sigma), pH 7.0, 10 mM magnesium sulfate, and 10% dimethyl sulfoxide (Sigma). The Coplin jars were then transferred to 25°C. Depending on the initial temperature of the fixative, times of fixation were 15 min (for 43°C) or 45 min for (20°C). After fixation, cells were washed with three 10-min incubations in 50 mM PIPES (pH 6.7).

Cell wall digestion was performed for 1 h at room temperature. The digestion solution contained Driselase (InterSpex Products, Foster City, CA) at 10.88 mg/ml, β-D-glucanase (InterSpex Products) at 64 mg/ml, and lyticase (ICN Biomedicals, Costa Mesa, CA) at 2 mg/ml in 50 mM sodium citrate, pH 5.8, with 50% (vol/vol) egg white. Before use, β-D-glucanase had been pretreated to reduce protease activity by heating a stock solution at 55°C for 5 min, incubating on ice for 30 min, and storing at −70°C (Ovechkina *et al.*, 1999). After digestion, coverslips were washed once for 5 min and twice for 10 min in 50 mM PIPES (pH 6.7). They were then incubated in −20°C methanol for 10 min and washed twice (5 and 10 min) in PE buffer (50 mM PIPES, pH 6.7, and 25 mM EGTA).

Immunofluorescence Microscopy

Coverslips were placed germling side down onto a 200–250-μl drop of solution, containing primary antibodies diluted in PE buffer with 0.5% of NP-40 (Sigma) and incubated for 1 h at room temperature. We used a mouse monoclonal anti-β-tubulin antibody (tu27b, originally obtained from Dr. Lester Binder, Northwestern University School of Medicine, Chicago, IL) and an affinity-purified rabbit polyclonal anti-γ-tubulin antibody (Oakley *et al.*, 1990). After four 10-min washes in PE buffer, coverslips were incubated overnight at 4°C in the dark on drops of secondary antibodies, diluted in the same buffer. Secondary antibodies had been preadsorbed against an *A. nidulans* acetone powder (Harlow and Lane, 1988) to decrease nonspecific binding. In double stainings, microtubules were always stained with fluorescein isothiocyanate or Alexa Fluor 488-conjugated goat-antimouse polyclonal secondary antibodies (Jackson Immunoresearch, West Grove, PA and Molecular Probes, Eugene, OR) and γ-tubulin with a Cy3-conjugated goat-antirabbit polyclonal secondary antibody (Jackson Immunoresearch).

After antibody staining, the cells were washed twice for 10 min and twice for 15 min in PE buffer and then postfixed with freshly prepared 2 mM [1-ethyl-3-(3-dimethylaminopropyl) carbodiimide hydrochloride] (Sigma) in PE buffer. Briefly, rinsed coverslips were

then stained in a 0.075 μg/ml 4′,6-diamidino-2-phenylindole (DAPI) (Sigma) solution, washed in water, and mounted with the antifade compound Citifluor AF1 (Marivac, Halifax, NS, Canada).

Image Acquisition and Preparation

Images were taken with a Nikon Eclipse E800 microscope (Nikon, Tokyo, Japan) equipped with a Princeton Instruments MicroMax charge-coupled device camera (Roper Scientific, Tucson, AZ) that was connected to a Power Macintosh personal computer. Images were acquired with the use of IPLab Spectrum software (Scanalytics, Fairfax, VA) and processed in NIH Image and Adobe Photoshop (Adobe Systems, Mountain View, CA). Composite pictures were prepared in CorelDraw 8 (Mac). All graphing was done in CricketGraph III on a Power Macintosh personal computer. Graphs were prepared for publication with the use of CorelDraw 8 (Corel Corporation, Ottawa, Ont).

Construction and Expression of a Maltose Binding Protein-KLPA Fusion

A full-length *klpA* cDNA was amplified by PCR from pKK12-29 (O'Connell *et al*., 1993). PCR primers were devised to produce *Bam*HI and *Xba*I sites at the ends of the amplified fragment. The amplified cDNA was ligated into the polylinker of pMAL-cRI (New England Biolabs, Beverly, MA) digested with *Bam*HI and *Xba*I, resulting in an in-frame fusion of the *klpA* open reading frame to the *malE* (maltose binding protein [MBP]) open reading frame. We designated the resulting plasmid pMAL-cRI-KLPA. For expression we transformed pMAL-cRI-KLPA into bacterial strain BL21 (DE3)pLysS (Promega, Madison, WI). For induction, cells were inoculated into medium containing 10 g/l tryptone, 5 g/l yeast extract, 5 g/l NaCl, and 2 g/l D-glucose supplemented with 50 μg/ml ampicillin and 34 μg/ml chloramphenicol. The culture was incubated at 37°C until an OD_{600} of ~0.5 was reached. Isopropyl β-D-thiogalactopyranoside was then added to a final concentration of 0.1 mM and the culture was incubated at 20°C for ~17.5 h. Cells were harvested by centrifugation and resuspended in 20 mM Tris, pH 7.4, 200 mM NaCl, 1 mM EGTA, and 1 mM $MgSO_4$. The suspension was frozen at −20°C. It was thawed to lyse the cells and a cleared supernatant was prepared by centrifugation at 6350 × *g* (r_{av}). The supernatant was then stored at −80°C until it was used.

Motility Assays

KLPA/MBP lysate was diluted 5- to 10-fold into 0.5× PM buffer (100 mM PIPES, 1 mM $MgSO_4$, 2 mM EGTA, pH 6.9) and 10 μl of diluted lysate was applied to a slide-coverslip chamber constructed with double-stick tape (Walker *et al*., 1997). After 3 min, unbound protein was washed out with 30 μl of 0.5× PM buffer then 10 μl of axoneme–microtubule complexes (Walker *et al*., 1990) or taxol-stabilized microtubules (25 μg/ml tubulin) containing MgATP was perfused into the chamber. Samples were immediately viewed by video-enhanced differential interference contrast microscopy and images were recorded on S-VHS videotape (Walker *et al*., 1997). An Argus 10 image processor (Hamamatsu, Bridgewater, NJ) was used to quantify gliding rates from the videotapes. Gliding rates are reported as mean ± SD.

RESULTS

Deletion of the klpA Gene Increases the Cold Sensitivity of Three mipA Alleles

We created double mutants carrying *klpA*1 (a deletion of the *klpA* gene; O'Connell *et al*., 1993) and conditionally lethal *mipA* alleles created by alanine scanning mutagenesis (Jung *et al*., 2001). *KlpA*1 is nearly silent (Figure 1) (restricting growth very slightly relative to the wild type), but we found that it dramatically increased the cold sensitivity of three *mipA* alleles, *mipA*D123 (a substitution of alanines for aspartic acid 123, arginine 124, and glutamic acid 125), *mipA*D159 (a substitution of alanines for aspartic acid 159 and arginine 160), and *mipA*H370 (a substitution of alanines for histidine 370 and arginine 371) and partially reduced the growth rates of these alleles even at permissive temperatures (Figure 1). We chose the *mipA*D123/*klpA*1 interaction for further study in preference to the other two double mutants for two reasons. First, *mipA*D159 is a tightly cold-sensitive mutant even without *klpA*1 and distinguishing the effects of *mipA*D159 from those caused by the synthetic interaction of *klpA*1 and *mipA*D159 is problematic. Second, the *mipA*H370/*klpA*1 double mutant is so cold sensitive that it is strongly inhibited for growth even at 37°C. The extreme cold sensitivity of this double mutant has prevented our creation of a *mipA*H370/*klpA*1/*nimT*23 triple mutant, which would be important for our phenotypic analyses (see below).

Effects of mipAD123 and klpA1 on Nuclear Division and Progression through Mitosis

Figure 1 shows the growth of strains carrying *mipA*D123 or *klpA*1, as well as the *mipA*D123/*klpA*1 double mutant at various temperatures. The double mutant is blocked for growth at 20°C and grows more slowly than either single mutant (*mipA*D123 or *klpA*1) at all temperatures. Because the growth rate of the *mipA*D123/*klpA*1 double mutant at low temperatures is much less than the growth rate of each single mutant, it follows that at least one essential process must be inhibited to a much greater extent in the double mutant at restrictive temperatures than in the single mutants. The microscopic phenotype of the double mutant at restrictive temperatures should reflect the inhibited essential functions and give valuable clues as to the nature of these essential functions.

Because phenotypes of unsynchronized material may reflect the cumulative effects of failed mitoses and not give a clear indication of the nature of the primary failure, we used a mutation, *nimT*23, to synchronize our mutants (Martin *et al*., 1997). *NimT* encodes a phosphatase (the homolog of the *S. pombe cdc25* phosphatase) that is essential for the activation of the *A. nidulans* homolog of $P34^{cdc2}$ (O'Connell *et al*., 1992). *NimT*23 is a heat-sensitive allele that blocks the cell cycle in G_2 at high temperatures (e.g., 43°C). Before germination, conidia are in G_1 and when conidia carrying *nimT*23 are germinated at 43°C, they proceed through the cell cycle until they are blocked in G_2. If they are then shifted to a permissive temperature, nuclei enter mitosis with excellent synchrony. For *mipA*D123 and *mipA*D123/*klpA*1, 43°C is a permissive temperature but 20°C is a restrictive temperature for both strains. Thus, by germinating spores at 43°C and shifting to 20°C, we could release the *nimT*23 block and simultaneously impose the *mipA*D123 or *mipA*D123/*klpA*1 block. Interestingly, we noted that *nimT*23 partially suppressed the growth restriction of the *mipA*D123/*klpA*1 double mutant at intermediate temperatures (Figure 1). This suppression is unlikely to affect our results because there was no suppression at the temperatures we used for our experiments, and the suppression did not affect the synchronization by *nimT*23, but this is an interesting phenomenon that may merit further study.

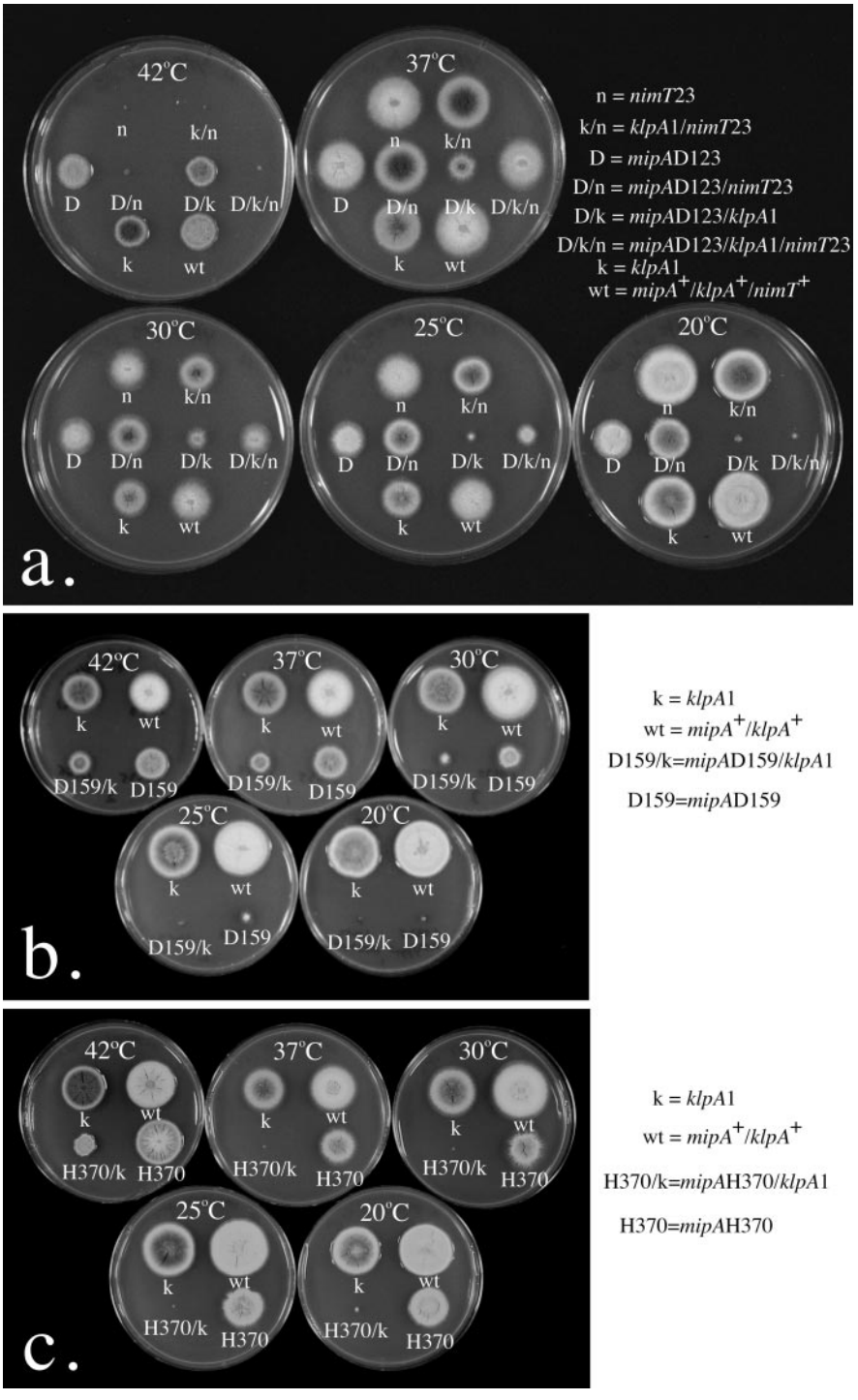

Figure 1. Synthetic interactions of *mipA* alleles with *klpA*1. Temperatures of incubation are shown at the top of each plate. Colonies grew from stab inocula of conidia, and colony diameter reflects growth rate. (a) At 20°C strains carrying *mipA*D123 and the wild-type *klpA* allele (D, D/n) are partially inhibited for growth relative to the wild-type control. Strains carrying *klpA*1 and the wild-type *mipA* allele (k, k/n) grow at a near normal rate, but growth of strains carrying both *mipA*D123 and *klpA*1 (D/k, D/k/n) are completely inhibited. At 25 and 30°C, all strains grow at near wild-type rates except for the strains carrying both *mipA*D123 and *klpA*1 (D/k, D/k/n). At 37°C, all strains except *mipA*D123/*klpA*1 (D/k) grow at near wild-type rates. Comparisons of the strain carrying *mipA*D123 and *klpA*1 (D/k) with the strain carrying *mipA*D123, *klpA*1, and *nimT*23 reveal that *nimT*23 partially suppresses the growth restriction conferred by the *mipA*D123/*klpA*1 combination at intermediate temperatures (25, 30, 37°C). Because *nimT*23 is heat sensitive none of the strains carrying *nimT*23 grow at 42°C. (b) Synthetic interaction of *mipA*D159 and *klpA*1. All strains are $nimT^+$ (c) Synthetic interaction of *mipA*H370 and *klpA*1. The double mutant hardly grows at 37°C or below and is partially inhibited at 42°C. All strains are $nimT^+$.

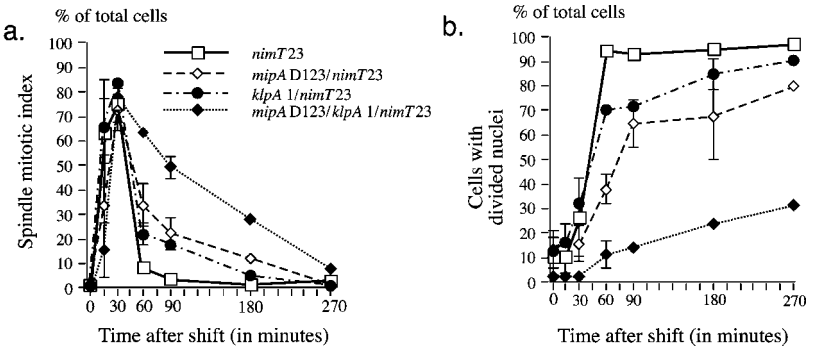

Figure 2. (a) Spindle mitotic index (percentage of germlings with mitotic spindles) in various strains after the shift from 43 to 20°C. All strains enter mitosis at about the same rate, but strains carrying *klpA*1 or *mipA*D123 remain in mitosis longer than the strain that is wild-type for these genes. Exit from mitosis is delayed to a still greater extent in the *klpA*1/*mipA*D123 double mutant. (b) Nuclear division (percentage of cells with two or more nuclei) after the shift to 20°C. Nuclear division was weakly inhibited in the strain carrying *klpA*1 and in the strain carrying *mipA*D123 but was much more strongly inhibited in the strain carrying both of these alleles. For both a and b, values represent mean ± SD for three separate experiments. Sample size for each strain for each time point was 400. Where bars are not shown, the SD was sufficiently small that the bars were within the symbol.

We first studied the effects of *mipA*D123 and *klpA*1, singly and in combination, on mitosis by analyzing the spindle mitotic index (SMI, the percentage of germlings with mitotic spindles [all spindle stages and morphologies are included in this percentage]) and by determining the fraction of germlings with two or more nuclei. As mentioned, nearly all germlings were blocked in G_2 of the first cell cycle (with 1 nucleus) until the shift to 20°C, and the presence of two or more nuclei after the shift indicated that nuclear division had occurred. As shown in Figure 2a, mutant strains entered mitosis rapidly and formed spindles at the same rate as the *mipA*+/*klpA*+/*nimT*23 strain, which served as the control. For brevity, we will refer to this strain as simply *nimT*23. Maximum SMIs of ~80% were achieved in all strains ~30 min after the shift to 20°C. Cell cycle time at 20°C is ~8 h (our unpublished results). There was, however, a significant difference in how control and mutant strains exited from mitosis. By 60 min after the shift, nearly all *nimT*23 germlings had interphase microtubule arrays and possessed two or more nuclei, most with interphase chromatin (data on chromatin condensation are our unpublished data), indicating a successful completion of mitosis (Figure 2b). *MipA*D123/*nimT*23 and *klpA*1/*nimT*23 germlings were slightly delayed in exiting mitosis, as judged by their spindle mitotic indices. Nevertheless, by 270 min (4.5 h) after the shift to 20°C all *klpA*1/*nimT*23 germlings had interphase microtubule arrays and ~90% of them possessed two or more nuclei. In *mipA*D123/*nimT*23 germlings, mitotic progression was slightly more inhibited due to a delay in anaphase progression (see below), but ~80% of all cells possessed two or more nuclei by 270 min after the shift. With *mipA*D123/*nimT*23 and *klpA*1/*nimT*23 strains the decrease in the SMI was gradual. This indicates that cells were not blocked with mitotic spindles for a precise length of time before they reentered interphase. Rather, the reentry appears to be probabilistic with some cells entering sooner than others.

In contrast to the wild type and both parental strains, the majority of *mipA*D123/klp*A*1/*nimT*23 germlings did not complete mitosis successfully. Mitotic spindles were present in many of the germlings long after mitosis had been completed in the *nimT*23 control and only ~30% of *mipA*D123/*klpA*1/*nimT*23 cells contained two or more nuclei 4.5 h after the shift to 20°C. These data indicate clearly that *mipA*D123 and *klpA*1 interact synthetically to inhibit nuclear division. *MipA*D123 and *klpA*1 each inhibit nuclear division slightly and the additive effects of the two mutations would be an ~25% inhibition relative to the *nimT*23 control. In combination, however, they cause a 65% inhibition relative to *nimT*23. In addition, a comparison of the spindle mitotic index data (Figure 2a) with nuclear division data (Figure 2b) reveals that most *mipA*D123/klp*A*1/*nimT*23 nuclei reenter interphase without dividing.

Inhibition of Bipolar Spindle Formation

The morphology of mitosis in *A. nidulans* is well studied and images of mitotic stages in wild-type cells have been published previously (Jung *et al.*, 1998, 2001). In *A. nidulans,* microtubules are absent from interphase nuclei. At the onset of mitosis, microtubules assemble from the adjacent SPBs and, at this point, the microtubules extending from the two SPBs are more or less parallel (Figure 8a). We will call this configuration "aster-like." In wild-type strains this aster-like configuration is very brief and spindles rapidly become bipolar and rod shaped. We see the aster-like configuration only occasionally in immunofluorescence microscopy of unsynchronized material, and observations of a green fluorescent protein-α-tubulin fusion show that it is very brief in living material (Maddox, Oakley, Salmon, and Oakley, unpublished data). Electron microscopy has revealed that, as spindles form, very short spindles with as few as 15 microtubules (as opposed to the 35–50 microtubules that are present in medial nuclear division spindles) are already bipolar (Oakley and Morris, 1983). We found that even in synchronized material the aster-like stage was not seen frequently. Fifteen minutes after the shift from 42 to 20°C, most of the *nimT*23 cells displayed very short but bipolar spindles and 7.5% had tiny aster-like spindles (Figure 3). In germlings carrying *mipA*D123, aster-like spindles were somewhat more abundant at the 15-min time point (~18% of germlings had such spindles), but all spindles had become bipolar by 30 min after the shift to 20°C. This suggests that *mipA*D123 may transiently delay the establishment of spindle bipolarity, but the effect is not large.

In *klpA*1/*nimT*23 cells, aster-like spindles were seen in much higher numbers (45% of germlings had aster-like spindles at 15 min after the shift), and they persisted for longer periods of time than in the *nimT*23 and *mipA*D123/*nimT*23 cells (Figure 3). In most cells, however, spindles apparently eventually became bipolar as the number of aster-like spindles decreased with time (Figure 3) and mitosis was com-

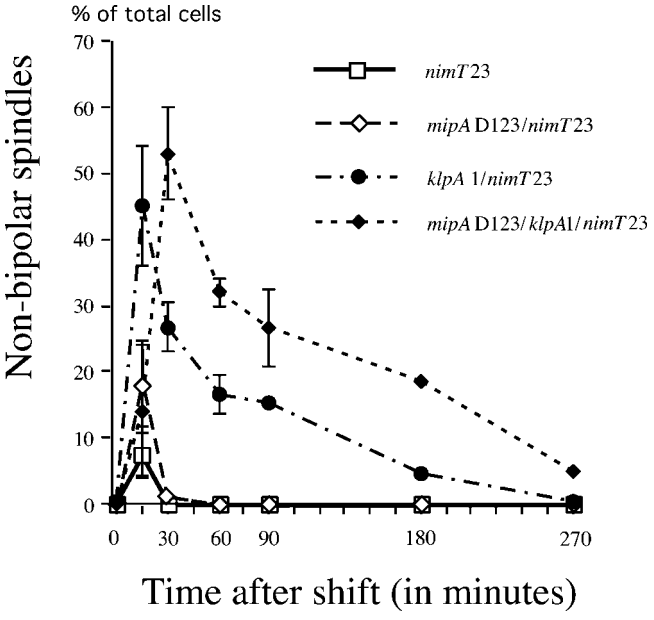

Figure 3. Percentage of germlings with aster-like, nonbipolar spindles (scored as a percentage of all germlings). Establishment of spindle bipolarity is slightly inhibited by *mipA*D123, more strongly inhibited by *klpA*1, and more strongly, still, by *mipA*D123 and *klpA*1 in combination. The inhibition by *mipA*D123 and *klpA*1 together is greater than the additive effects of the two mutations. Values represent mean ± SD for three separate experiments. Sample size for each experiment was 400 cells. Where bars are not shown, the SD was sufficiently small that the bars were within the symbol.

pleted successfully (Figure 2b). By 1 h after the shift, most cells had successfully completed mitosis and possessed two or more nuclei. Practically all spindles remaining after this point were aster-like. Even more nonbipolar, aster-like spindles were seen in germlings carrying both *mipA*D123 and *klpA*1 (*mipA*D123/*klpA*1/*nimT*23) and they persisted longer than in the germlings that carried *klpA*1 without *mipA*D123 (Figure 3). Representative images of nonbipolar spindles in a *mipA*D123/*klpA*1/*nimT*23 strain are shown in Figure 4.

MipAD123 Inhibits the Completion of Anaphase A, but klpA1 neither Inhibits Anaphase A nor Increases the Inhibition Conferred by mipAD123

In *A. nidulans*, before anaphase A the chromosomes never align at a metaphase plate but are usually in an irregular clump. In anaphase A they move to the poles, forming a clump of chromatin at each pole (Jung *et al.*, 1998, and references therein). During anaphase A, chromosomes may be transiently arranged along the spindle, but anaphase A normally occurs very quickly and such configurations are not seen frequently in unsynchronized material. In strains carrying *mipA*D123, we observed that, starting at ~60 min after the shift to 20°C, a large percentage of the spindles were elongate with chromosomes arranged along the spindle (Figures 4 and 5). Such spindles were extremely rare in *nimT*23 and *klpA*1/*nimT*23 strains. These results indicate that *mipA*D123 substantially inhibits completion of anaphase A. If we look at the frequencies of the various spindle morphologies in *mipA*D123/*nimT*23 and *mipA*D123/*klpA*1/*nimT*23 (Figure 6, a and b), it is apparent that the establishment of spindle bipolarity is dramatically inhibited in *mipA*D123/*klpA*1/*nimT*23, but spindles that do become bipolar are inhibited in completion of anaphase A to about the same extent as spindles in *mipA*D123/*nimT*23. *KlpA*1 thus does not appear to have any effect on the completion of anaphase A.

KLPA Is a Minus-End–directed Motor

Circumstantial evidence suggests that KLPA should be a minus-end–directed motor protein. First, all C-terminal kinesin motors examined to date (Ncd, Kar3p, and KCBP; McDonald *et al.*, 1990; Walker *et al.*, 1990; Endow *et al.*, 1994; Song *et al.*, 1997) have been shown to move toward the minus end of microtubules. Second, KLPA, like these motor proteins, contains the minus end-directed neck motif (Endow and Waligora, 1998). Understanding the function of KLPA in spindle assembly requires knowledge of the directionality of the motor. To determine the direction of KLPA movement, we expressed a KLPA/MBP fusion in *E. coli*, and used video-enhanced differential interference light microscopy to examine the motile properties of this protein. Because purification was found to render the protein inactive, motility assays were performed with clarified lysates prepared from KLPA/MPB-expressing cells. Axoneme–microtubule complexes were observed to glide across KLPA/MBP-coated coverslip surfaces with the microtubule end (plus end) leading (Figure 7a), demonstrating that KLPA moves toward the microtubule minus end. The rate of axoneme–microtubule complex gliding in the presence of 1 mM MgATP was 10.7 ± 2.4 μm/min (n = 18). In comparison, taxol-stabilized microtubules moved at 15.1 ± 2.1 μm/min (n = 30) in the presence of 1 mM MgATP. Higher concentrations of MgATP caused a slight increase in gliding rate for taxol-stabilized microtubules. The rate of gliding for 5 mM and 10 mM MgATP was 17.4 ± 2.1 μm/min (n = 30) and 17.7 ± 1.7 μm/min (n = 30), respectively. The relatively small change in rate between 5 and 10 mM MgATP suggests that the maximum rate for KLPA is ~18 μm/min. This rate is the fastest reported so far for a C-terminal motor domain kinesin but is only slightly faster than the rate reported for Ncd (McDonald *et al.*, 1990). In addition to gliding activity, KLPA/MPB preparations also demonstrated microtubule bundling activity (Figure 7b). Large tangled bundles of microtubules were commonly observed and occasionally adjacent microtubules could be seen to zip and unzip along their lengths. We did not detect any microtubule depolymerization during our experiments.

DISCUSSION

We have found that *klpA*1, a nearly silent deletion of the gene that encodes a C-terminal motor domain kinesin-like protein in *A. nidulans*, dramatically increases the cold sensitivity of three γ-tubulin alleles. A γ-tubulin mutation of *S. pombe*, *gtb1*-PL301, is synthetically lethal with a deletion of the *pkl1* gene, which also encodes a C-terminal motor domain kinesin-like protein (Paluh *et al.*, 2000). Our data reveal that such interactions are not specific to *S. pombe* but are more general. In addition, because our double mutants are not dead, but cold sensitive, we were able to examine the

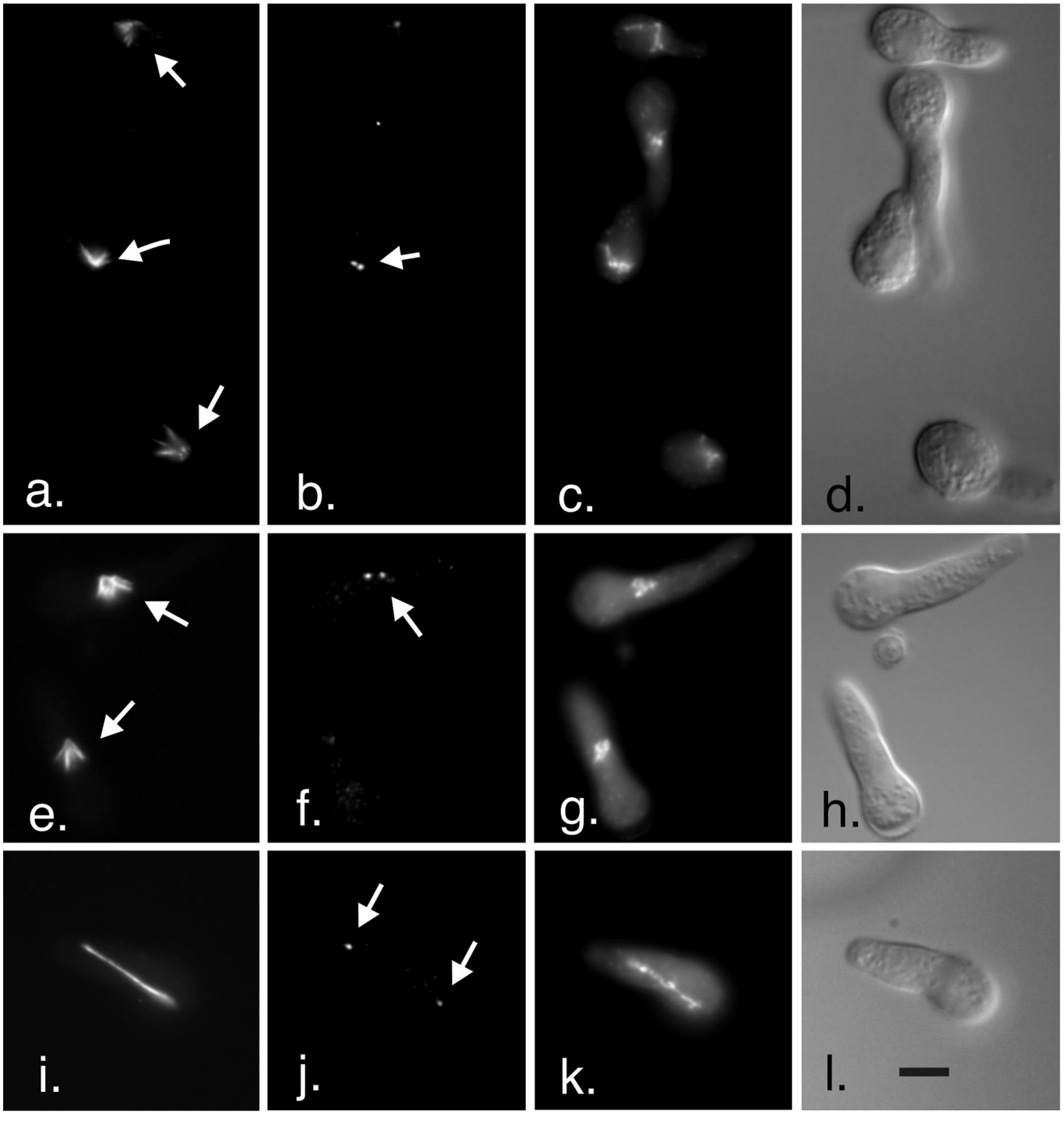

Figure 4. Representative microtubule, γ-tubulin, and chromatin arrangements in *mipA*D123/*klpA*1/*nimT*23. (a–d) Material fixed 15 min after the shift to 20°C. Four germlings are visible and three have nonbipolar spindles (arrows in a). (b) γ-Tubulin staining. γ-Tubulin staining of SPBs is visible in three of the germlings and is out of the plane of focus in the bottom germling. In one of the germlings the replicated but barely separated SPBs are visible as two γ-tubulin–stained spots (arrow in b). (c and d) DAPI and differential interference contrast images of the same field. (e–h) Two germlings fixed at 30 min after the shift. Nonbipolar spindles are present in both germlings (arrows in e). γ-Tubulin staining shows that the SPBs have separated slightly in the upper germling (arrow in f). The SPBs for the lower germling are out of the plane of focus. (g and h) DAPI and differential interference contrast images of the same field. (j–l) Germling fixed at 90 min after the shift. The spindle (i) is elongated. γ-Tubulin staining is present at the poles of the spindles (arrows in j) but the chromosomes have not moved to the poles (k). All images are the same magnification. Bar in l, 5 μm.

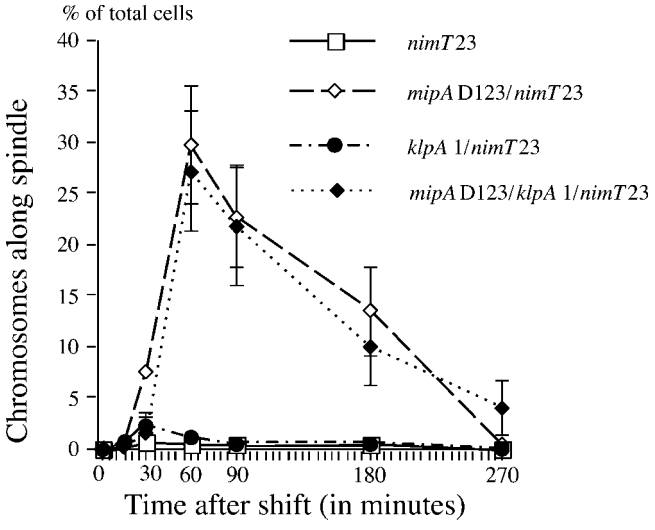

Figure 5. Percentage of total germlings that have chromosomes positioned along a bipolar mitotic spindle. Chromosomes do not form a metaphase plate in *A. nidulans*, and the fact that chromosomes are positioned along the spindle indicates that chromosomes have not segregated to the poles and thus that anaphase A has not been completed successfully. Values represent means ± SDs for three separate experiments. Sample size at each time point for each experiment was 400. Where bars are not shown, the SD was sufficiently small that the bars were within the symbol.

phenotype of one of the double mutants and this has allowed us to begin to understand the essential processes inhibited in the double mutant. In particular, the precise synchronization afforded by *nimT*23 has allowed us to examine the effects on mitotic progression of *mipA*D123 and *klpA*1, separately and together.

Separately, *klpA*1 causes a substantial but transient delay in the establishment of spindle bipolarity, whereas *mipA*D123 causes a delay in anaphase A, chromosome movement to the mitotic poles. The *S. pombe* γ-tubulin mutation *gtb1*-PL301 also inhibits anaphase A (Paluh *et al.*, 2000), and our data reveal that such an inhibition is not limited to *gtb1*-PL301 or to *S. pombe* but is a more general characteristic of γ-tubulin mutations. In strains carrying both mutations, *mipA*D123 exacerbates the spindle bipolarity defect of *klpA*1 such that more aster-like spindles are seen. It also takes them longer to become bipolar and many apparently never become bipolar before reentering interphase. *KlpA*1, on the other hand, seems to have little effect on the inhibition of anaphase A caused by *mipA*D123.

What is the nature of the synthetic interaction? It is important to remember that *klpA*1 is a deletion. The synthetic interaction, thus, does not imply that there is a physical interaction between γ-tubulin and KLPA. Rather, it implies that γ-tubulin and KLPA are essential components of two redundant pathways, either of which can enable spindles to become bipolar. The pathway involving KLPA appears to be the primary pathway because *klpA*1 on its own causes a significant delay in spindle bipolarity. The pathway that involves γ-tubulin appears to be secondary because *mipA*D123 causes only a slight inhibition of spindle bipolarity on its own. When the KLPA pathway is inhibited, however, the pathway involving γ-tubulin eventually rescues the aster-like spindles and allows them to become bipolar. When both pathways are inhibited (i.e., in the double mutant) the establishment of spindle bipolarity is sufficiently inhibited such that most spindles never become bipolar and never successfully complete mitosis.

In view of the fact that the C-terminal motor domain kinesin-like protein Ncd is involved in movement of γ-tubulin to a microtubule organizing center (Endow and Komma, 1998), we considered the possibility that KLPA might be involved in transporting γ-tubulin to the SPB. Our evidence suggests that this is not likely. Immunofluorescence microscopy shows clearly that γ-tubulin localizes to the SPB in *klpA*1 strains (both *mipA*+ and *mipA*D123). The *klpA*1 single mutant grows at nearly normal rates so it is safe to assume that adequate amounts of γ-tubulin are present at the SPB in this strain. It is also important to remember that in our synchronization experiments, strains were initially incubated at 43°C, which is a permissive temperature for the *mipA*D123/*klpA*1 double mutant. Because the double mutant grows well at this temperature, we can assume that adequate amounts of γ-tubulin must be transported to the SPB in the double mutant at this temperature. Mitosis began shortly after the shift to 20°C, and it is unlikely that γ-tubulin would have been removed from the SPB in this interval.

Because γ-tubulin has a now well established role in microtubule nucleation (reviewed by Wiese and Zheng, 1999; Oakley, 2000), we considered the possibility that the synthetic lethality was due to inhibition of microtubule nucleation. Our data and previous findings suggest that this is unlikely. Immunofluorescence microscopy gives no indication that microtu-

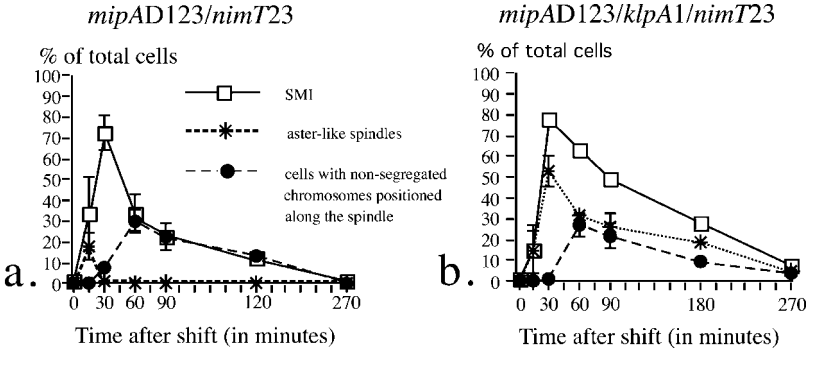

Figure 6. Frequencies of mitotic spindle types. In the *mipA*D123/*nimT*23 strain (a), there is a transient inhibition of the establishment of spindle bipolarity, resulting in a small percentage of aster-like spindles. By 30 min after the shift from 43 to 20°C, all spindles are bipolar. Anaphase A is inhibited in many germlings, however, such that by 60 min after the shift, chromosomes are arranged along nearly all of the remaining spindles. In the *mipA*D123/*klpA*1/*nimT*23 strain (b), there is a substantial inhibition of the establishment of spindle bipolarity, resulting in a high frequency of aster-like spindles. Some spindles become bipolar but these are inhibited in anaphase A. By 60 min after the shift, nearly all spindles are either aster-like or have chromosomes positioned along them.

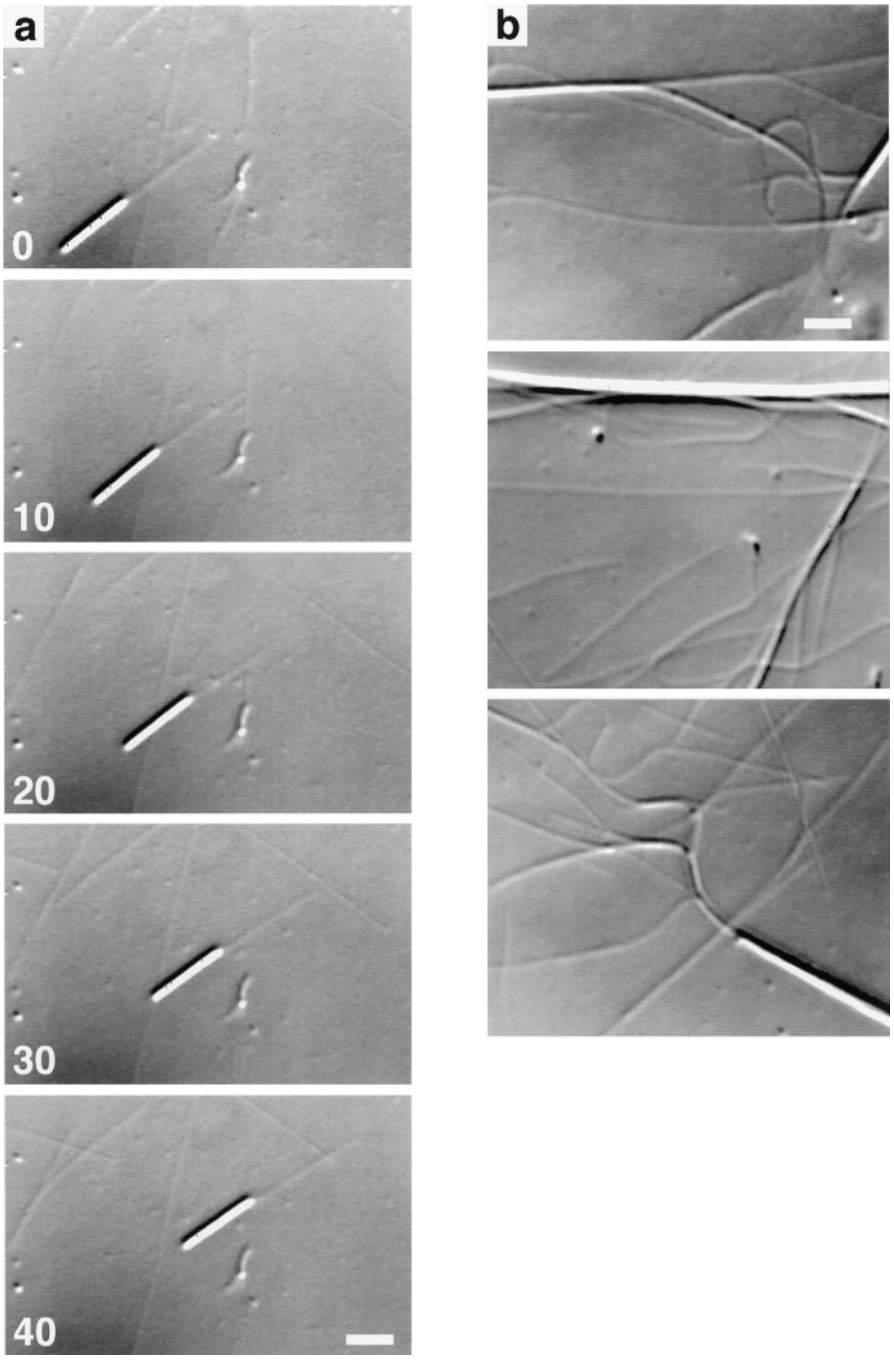

Figure 7. KLPA is a minus-end–directed motor protein that bundles microtubules. (a) Axonemes with microtubules assembled only from the plus ends were prepared as described (Walker *et al.*, 1990), mixed with MgATP (1 mM final concentration), and applied to a coverslip coated with bacterial cell lysate containing the KLPA/MBP fusion protein. This figure shows gliding of an axoneme–microtubule complex with the microtubule end (i.e., the plus end) of the complex leading. This indicates that the motor is moving toward the axoneme (minus) end of the complex. Time in seconds is indicated at the lower left of each panel (bar, 2 μm). (b) Three different fields from microtubule gliding assays with 1 mM MgATP demonstrate the bundling activity of KLPA/MBP. No axonemes are present in these samples and few individual microtubules can be observed. Most microtubules have bundled to form thicker, higher contrast structures. Bar, 2 μm.

bule assembly is inhibited. We cannot rule out the possibility that there is some partial inhibition, but this would not account for the major defect we observe in the double mutant, i.e., the failure of spindles to become bipolar. Electron microscopy has shown that spindles can become bipolar when only a few microtubules are present (Oakley and Morris, 1983).

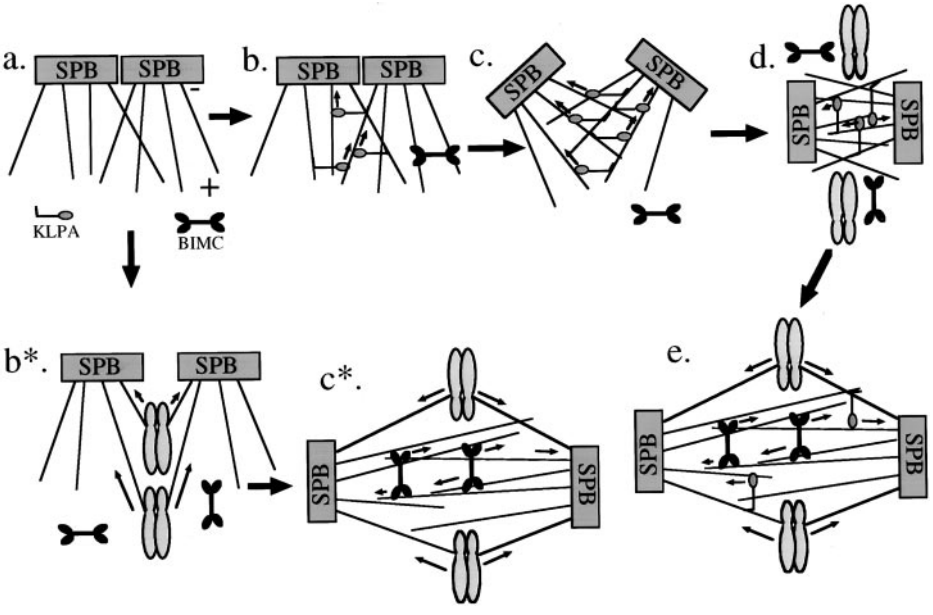

Figure 8. Model for the establishment of spindle bipolarity in *A. nidulans*. (a) Microtubules grow from adjacent SPBs and are more or less parallel. (b) When KLPA is present, the nonmotor microtubule binding domain will bind to microtubules and if the motor domain interacts with a microtubule extending from the other SPB, it will move down the microtubule toward the minus end at the SPB. This will pull the microtubules and SPBs into a bipolar configuration (c and d). Interactions of KLPA with two microtubules from the same SPB will not be productive and are not shown. BIMC can bind to microtubules at this point but because they are parallel, BIMC would simply move to the plus end and, presumably, fall off the microtubule. Once bipolarity is established, however, BIMC binding to antiparallel microtubules would crosslink microtubules and provide a force to push the poles apart (e). This force would offset the force produced by KLPA. In the absence of KLPA, another force must pull the spindle into a bipolar configuration. We postulate that this force is provided by motors at the kinetochore pulling on kinetochore microtubules (b*). Eventually a bipolar spindle is formed where the poleward forces produced by the kinetochore motors are in balance with the forces produced by BIMC (c*).

In discussing the nature of the synthetic lethality, it is useful to discuss the phenotype conferred by *klpA*1 alone. We believe, moreover, that this phenotype is important for understanding the role of C-terminal motor domain kinesins independent of any interaction with γ-tubulin. One surprise was that the transient aster-like spindles caused by *klpA*1 were at least superficially similar to the aberrant spindles caused by *bimC*4, a heat-sensitive mutation in *A. nidulans*. *BimC* encodes a kinesin that is apparently required for spindle elongation and maintenance of spindle bipolarity. *KlpA*1 partially suppresses the heat sensitivity conferred by *bimC*4, and it was a surprise that *klpA*1 causes, at least transiently, a phenotype similar to that of the mutation it suppresses. It was also a surprise that the phenotype of *klpA*1 is similar to the phenotype of KLPA overexpression (aberrant monopolar spindles) (O'Connell *et al.*, 1993).

We have devised a model (Figure 8) to explain our results. At the beginning of spindle formation, SPBs are side by side and microtubules are more or less parallel (Figure 8a). For spindles to become bipolar, something has to push or pull such that the microtubules from the two spindle poles become oriented in an antiparallel manner. KLPA is part of one of two redundant mechanisms that do this. From our in vitro data we can deduce that KLPA has two microtubule binding domains, a motor domain and a nonmotor domain. If a nonmotor domain binds to a microtubule, the motor domain will generate movement toward the minus end of any microtubule that it encounters. If it encounters a microtubule from the same spindle pole, the interaction will not be productive. It will simply generate a transient shear force between the two microtubules. If it encounters a microtubule from the other spindle pole, it will move down the microtubule toward the other spindle pole. This will pull the microtubules into an antiparallel arrangement (Figure 8, b and c). If the nonmotor domain of a KLPA molecule fails to bind to a microtubule, the molecule would rapidly move to the minus end of the microtubule at the SPB. This would cause KLPA to accumulate at the SPB, but the SPB would not be the site of action.

BIMC is the founding member of a family of tetrameric kinesins (reviewed by Sharp *et al.*, 2000) involved in spindle elongation. These kinesins generate shear forces between antiparallel microtubules. Before the establishment of spindle bipolarity BIMC molecules would bind to microtubules and simply move to the plus ends and fall off. As originally suggested by Enos and Morris (1990), when bipolarity is established BIMC molecules are able to bind to antiparallel microtubules and exert force pushing the poles apart (Figure 8d). BIMC would thus not be sufficient to establish spindle bipolarity in *A. nidulans* but would be important for the maintenance of bipolarity once it is established.

In the absence of KLPA, a second, less efficient mechanism establishes spindle bipolarity. We suggest that poleward forces exerted at the kinetochores pull the spindle into an antiparallel configuration (Figure 8, b* and c*). Our results show that *mipA*D123 inhibits anaphase A, and this suggests that *mipA*D123 somehow inhibits force production or transmission at the kinetochore. Although it is possible that the synthetic interaction of *mipA*D123 with *klpA*1 is unrelated to the effects of *mipA*D123 on chromosomal movement, the inhibition of poleward forces at the kinetochore by *mipA*D123 would provide a parsimonious explanation for inhibition of anaphase A and inhibition of the establishment of spindle bipolarity. It is also worth noting that *mipA*D159, which is also synthetically lethal with *klpA*1, inhibits anaphase A (our unpublished data), and that the *S. pombe* mutation *gtb1*-PL301, which is synthetically lethal with a

deletion of the C-terminal motor domain kinesin-like protein Pkl1p, also inhibits anaphase A (Paluh *et al.*, 2000).

How could *mipA*D123 affect force production at the kinetochore given that most, if not all, γ-tubulin in the spindle is at the SPB? One obvious possibility is that *mipA*D123 weakens the attachment of microtubules to the SPB. Kinetochores pulling on kinetochore microtubules might break the kinetochore microtubules free from the SPB, causing the loss of poleward force. We believe that this is a reasonable possibility, but we would expect that if such a mechanism were operating, it would cause a greater inhibition of mitosis and growth in the *mipA*D123 single mutant than we observe.

A second possibility is that small amounts of γ-tubulin at the kinetochore or elsewhere in the spindle, difficult to detect by immunofluorescence, are involved in regulating force production at the kinetochore. This would be consistent with the localization of γ-tubulin to the mitotic spindles of some organisms, but at present there are no experimental data that support or rule out this hypothesis.

A third possibility that initially appealed to us is that microtubule flux (addition of tubulin dimers at the kinetochore and removal at the SPB) might create a poleward force at the kinetochore that is required, directly or indirectly, for anaphase A. A γ-tubulin mutation might, reasonably, be expected to inhibit subunit removal at the SPB, and thus inhibit anaphase A. We have looked vigorously for evidence of flux in wild-type strains with the use of the fluorescence recovery after photobleaching technique, but repeated experiments have given no evidence that flux occurs in *A. nidulans* spindles (Maddox, Oakley, Salmon, and Oakley, unpublished data). We cannot rule out the possibility that flux occurs in a small but important subset of spindle microtubules so it remains formally possible (although perhaps unlikely) that *mipA*D123 inhibits mitosis by inhibiting flux.

A fourth possibility is that γ-tubulin has a role in a signal transduction pathway that activates a kinetochore motor. Signal transduction pathways clearly operate in mitosis although they are incompletely understood. The most obvious example is checkpoint regulation, but logic and experimental evidence indicate that precise regulation of motor protein activity is required for successful mitotic progression (Sharp *et al.*, 2000). A direct link between checkpoint regulation and γ-tubulin function is provided, moreover, by data from *S. pombe* (Paluh *et al.*, 2000). As mentioned, the *S. pombe* γ-tubulin mutation *gtb1*-PL301 is synthetically lethal with a deletion of the gene that encodes the C-terminal kinesin-like protein Pkl1p. Separated from the *pkl1* deletion, *gtb1*-PL301 is cold sensitive and inhibits anaphase A at restrictive temperatures. A disruption of the checkpoint regulatory gene *mad2*, however, suppresses the cold sensitivity conferred by *gtb1*-PL301, relieving the anaphase A block and restoring growth. Although there are other possible explanations (Paluh *et al.*, 2000), we believe the simplest explanation for these data is that *gtb1*-PL301 inhibits anaphase A by causing an inappropriate checkpoint blockage. The spindle is capable of moving chromosomes to the poles, but the checkpoint block prevents it from doing so. The *mad2* disruption removes the checkpoint block, spindles move the chromosomes to the poles, mitosis is completed, and cells replicate at a near normal rate. If the spindles were incapable of producing proper chromosomal movement, one would expect the *mad2* disruption to cause mitotic failures and exacerbate any growth defect rather than suppress it. This explanation implies that γ-tubulin has a role in checkpoint regulation. Given its position at the minus end of the microtubules and its role in microtubule nucleation, it is certainly possible that a checkpoint regulatory mechanism might monitor γ-tubulin occupancy (presence or absence of microtubules attached to γ-tubulin) as part of mechanism for testing spindle integrity.

Although *gtb1-PL301* and *mipA*D123 are in different portions of the γ-tubulin molecule (*mipA*D123 is in the helix 3 region [Jung *et al.*, 2001] and *gtb1*-PL301 is in the region between helix 9 and β-sheet 8 [Paluh *et al.*, 2000]), the phenotypes of these mutations are similar. Both display strong synthetic interactions with deletions of C-terminal motor domain kinesin-like proteins and both inhibit anaphase A.

Our model seems to be in agreement with most or all of the findings made with KLPA and related proteins in *A. nidulans*. Overexpression of KLPA would increase the forces pulling SPBs together, causing spindle collapse and small dysfunctional spindles similar to the phenotype observed by O'Connell *et al.* (1993). Inactivation of BIMC (as with *bimC*4 at restrictive temperatures) would cause a similar imbalance of forces and a similar phenotype and this is the case (Enos and Morris, 1990). It is worth noting that the prediction for inactive BIMC is that as nuclei enter mitosis there would initially be a short bipolar spindle with SPBs very close together (similar to Figure 8c), but if KLPA were inactivated over time (as probably happens when normal spindles enter anaphase), bipolarity would be lost. Inactivation or absence of KLPA would be predicted to reduce spindle collapse caused by lack of active BIMC. This might account for the partial suppression of *bimC*4 by *klpA*1 (O'Connell *et al.*, 1993) and would imply that there is a second mechanism for spindle elongation that does not require BIMC. Observations on living material suggest that such a mechanism may involve forces exerted on the SPBs through cytoplasmic microtubules (Maddox, Oakley, Salmon, and Oakley, unpublished data).

Our model is similar to previous models for C-terminal kinesin-like protein functions (Saunders and Hoyt, 1992; O'Connell *et al.*, 1993; Pidoux *et al.*, 1996; reviewed by Sharp *et al.*, 2000) in that we suggest that KLPA cross-bridges microtubules from opposite poles and provides a force that pulls poles together. It differs from most other models in several ways, however. First, we suggest that the minus-end–directed motor activity and microtubule binding activity of KLPA allow it to pull the spindle into a bipolar configuration. This is an important function in fungi and other organisms in which the microtubules that extend from the microtubule organizing centers are initially parallel and have to be moved into an antiparallel arrangement. Second, we suggest that a second mechanism by which spindle bipolarity is established involves poleward forces acting on the kinetochore. It is clear from many observations that KLPA and other C-terminal motor domain kinesin-like proteins are not essential for cellular growth and reproduction. There are thus other mechanisms that carry out all the functions of KLPA and related proteins. Our data suggest that at least one of those mechanisms involves forces acting at kinetochores. Third, our model suggests that KLPA and related proteins need not function at poles even although they accumulate there. Because the minus ends of spindle

microtubules are at the poles, any minus-end–directed motor will tend to accumulate at the poles, regardless of whether it functions at the poles.

Although we do not wish to engage in a comprehensive discussion of mitotic motor proteins, our model also seems to be generally consistent with observations in *S. cerevisiae*, *S. pombe*, and *D. melanogaster* (discussed in INTRODUCTION). In particular, it explains the partial inhibition of spindle bipolarity caused by inactivation of Kar3p and Kip3p (Cottingham *et al.*, 1999) as well as the spindle collapse caused by overexpression and the suppression of mutations of BIMC family members.

Mutations in BIMC family kinesins have been shown to cause unipolar spindles with unseparated SPBs in *A. nidulans* (Enos and Morris, 1990), *S. pombe* (Hagan and Yanagida, 1992) and *S. cerevisiae* (Hoyt *et al.*, 1992; Roof *et al.*, 1992). These findings have led to the suggestion that the BIMC family kinesins mediate SPB separation and migration to form bipolar spindles (Hagan and Yanagida, 1992; Roof *et al.*, 1992). Our data demonstrate that the establishment of spindle bipolarity is strongly inhibited in *mipA*D123/*klpA*1 strains even if they carry no *bimC* mutation. This reveals that functional BIMC is not sufficient to allow normal establishment of spindle bipolarity. Although it is possible that there are species-specific variations in BIMC family function, our data suggest that the real functions of BIMC family kinesins are to stabilize spindle bipolarity and elongate the spindle. Mutational inactivation of BIMC family kinesins can result in a configuration in which SPBs are side by side and microtubules are in a parallel configuration similar to Figure 8b (Hoyt *et al.*, 1992; Roof *et al.*, 1992; Oakley and Morris, unpublished data). Although these data suggest, at face value, that BIMC family kinesins are involved in establishing spindle bipolarity, there are at least two interpretations of these results that are consistent with our model. First, KLPA and related kinesin-like proteins may be unable to stabilize a bipolar configuration in the absence of functional BIMC family members. Second, KLPA family members may become inactivated with time and, in the absence of a BIMC family member to stabilize the bipolar spindle, this allows short bipolar spindles to collapse into the nonbipolar configuration observed.

Our model does not address the suppression of KAR3 mutations by benomyl nor does it address nonmitotic functions of C-terminal motor domain kinesins. We find that the growth inhibition of *mipA*D123/*klpA*1 strains is slightly suppressed by benomyl and nocodazole (our unpublished data). This may indicate that a small fraction of the growth inhibition has to do (directly or indirectly) with microtubule assembly or dynamics, but most of the effects we see appear to be independent of these phenomena. Our model does not fully explain the observations on *KAR3* and *SLK19* in *S. cerevisiae* (Zeng *et al.*, 1999), but it does at least provide a framework for understanding how mutations in genes that encode kinetochore proteins might interact genetically with *KAR3*.

ACKNOWLEDGMENTS

We thank Qi Ma for helping with *mipA*D123/*klpA*1 crosses, Luh Tung for help in constructing pMAL-cRI-KLPA, Liang Yi for helping develop expression conditions, and Michael Claybon for expressing the MBP/KLPA fusion. We thank Dr. N.R. Morris for a strain carrying *klpA*1 and Dr. Matthew O'Connell for plasmid pKK12–29. This study was supported by grants GM-31837 from the National Institutes of Health to B.R.O. and GM-52340 to R.A.W.

REFERENCES

Cottingham, F.R., Gheber, L., Miller, D.L., and Hoyt, M.A. (1999). Novel roles for *Saccharomyces cerevisiae* mitotic spindle motors. J. Cell Biol. *147*, 335–349.

Endow, S.A., Kang, S.J., Satterwhite, L.L., Rose, M.D., Skeen, V.P., and Salmon, E.D. (1994). Yeast Kar3 is a minus-end microtubule motor protein that destabilizes microtubules preferentially at the minus ends. EMBO J. *13*, 2708–2713.

Endow, S.A., and Komma, D.J. (1998). Assembly and dynamics of an anastral:astral spindle: the meiosis II spindle of *Drosophila* oocytes. J. Cell Sci. *111*, 2487–2495.

Endow, S.A., and Waligora, K.W. (1998). Determinants of kinesin motor polarity. Science *281*, 1200–1202.

Enos, A.P., and Morris, N.R. (1990). Mutation of a gene that encodes a kinesin-like protein blocks nuclear division in *A. nidulans*. Cell *60*, 1019–1027.

Hagan, I., and Yanagida, M. (1992). Kinesin-related cut7 protein associates with mitotic and meiotic spindles in fission yeast. Nature *356*, 74–76.

Hoyt, M.A., He, L., Loo, K.K., and Saunders, W.S. (1992). Two *Saccharomyces cerevisiae* kinesin-related gene products required for mitotic spindle assembly. J. Cell Biol. *118*, 109–120.

Hoyt, M.A., He, L., Totis, L., and Saunders, W.S. (1993). Loss of function of *Saccharomyces cerevisiae* kinesin-related *CIN8* and *KIP1* is suppressed by *KAR3* motor domain mutations. Genetics *135*, 35–44.

Jung, M.K., May, G.S., and Oakley, B.R. (1998). Mitosis in wild-type and β-tubulin mutant strains of *Aspergillus nidulans*. Fungal Genet. Biol. *24*, 146–160.

Jung, M.K., Prigozhina, N., Oakley, C.E., Nogales, E., and Oakley, B.R. (2001). Alanine-scanning mutagenesis of *Aspergillus* γ-tubulin yields diverse and novel phenotypes. Mol. Biol. Cell *12*, 2119–2136.

Martin, M.A., Osmani, S.A., and Oakley, B.R. (1997). The role of γ-tubulin in mitotic spindle formation and cell cycle progression in *Aspergillus nidulans*. J. Cell Sci. *110*, 623–633.

Matthies, H.J.G., McDonald, H.B., Goldstein, L.S.B., and Theurkauf, W.E. (1996). Anastral meiotic spindle morphogenesis: role of the non-claret disjunctional kinesin-like protein. J. Cell Biol. *134*, 455–464.

McDonald, H.B., Stewart, R.J., and Goldstein, L.S.B. (1990). The kinesin-like *ncd* protein of Drosophila is a minus end-directed microtubule motor. Cell *63*, 1159–1165.

Meluh, P.B., and Rose, M.D. (1990). *KAR3*, a kinesin-related gene required for yeast nuclear fusion. Cell *60*, 1029–1041.

O'Connell, M.J., Meluh, P.B., Rose, M.D., and Morris, N.R. (1993). Suppression of the *bimC*4 mitotic spindle defect by deletion of *klpA*, a gene encoding a KAR3-related kinesin-like protein in *Aspergillus nidulans*. J. Cell Biol. *120*, 153–162.

O'Connell, M.J., Osmani, A.H., Morris, N.R., and Osmani, S.A. (1992). An extra copy of *nim*E^{cyclinB} elevates pre-MPF levels and partially suppresses mutation of *nim*T^{cdc25} in *Aspergillus nidulans*. EMBO J. *11*, 2139–2149.

Oakley, B.R. (2000). γ-Tubulin. Curr. Top. Dev. Biol. *49*, 27–54.

Oakley, B.R., and Morris, N.R. (1983). A mutation in *Aspergillus nidulans* that blocks the transition from interphase to prophase. J. Cell Biol. *96*, 1155–1158.

Oakley, B.R., Oakley, C.E., Yoon, Y., and Jung, M.K. (1990). γ-Tubulin is a component of the spindle-pole-body that is essential for microtubule function in *Aspergillus nidulans*. Cell *61*, 1289–1301.

Ovechkina, Y.Y., Pettit, R.K., Cichacz, Z.A., Pettit, G.R., and Oakley, B.R. (1999). Unusual antimicrotubule activity of the antifungal agent spongistatin 1. Antimicrob. Agents Chemother. *43*, 1993–1999.

Paluh, J.L., Nogales, E., Oakley, B.R., McDonald, K., Pidoux, A., and Cande, W.Z. (2000). A mutation in γ-tubulin alters microtubule dynamics and organization and is synthetically lethal with the kinesin-like protein Pkl1p. Mol. Biol. Cell *11*, 1225–1239.

Pidoux, A.L., LeDizet, M., and Cande, W.Z. (1996). Fission yeast pkl1 is a kinesin-related protein involved in mitotic spindle function. Mol. Biol. Cell *7*, 1639–1655.

Roof, D.M., Meluh, P.B., and Rose, M.D. (1992). Kinesin-related proteins required for assembly of the mitotic spindle. J. Cell Biol. *118*, 95–108.

Saunders, W., Hornack, D., Lengyel, V., and Deng, C. (1997a). The *Saccharomyces cerevisiae* kinesin-related motor Kar3p acts at preanaphase spindle poles to limit the number and length of cytoplasmic microtubules. J. Cell Biol. *137*, 417–431.

Saunders, W., Lengyel, V., and Hoyt, M.A. (1997b). Mitotic spindle function in *Saccharomyces cerevisiae* requires a balance between different types of kinesin-related motors. Mol. Biol. Cell *8*, 1025–1033.

Saunders, W.S., and Hoyt, M.A. (1992). Kinesin-related proteins required for structural integrity of the mitotic spindle. Cell *70*, 451–458.

Sharp, D.J., Rogers, G.C., and Scholey, J.M. (2000). Microtubule motors in mitosis. Nature *407*, 41–47.

Song, H., Golovkin, M., Reddy, A.S.N., and Endow, S.A. (1997). In vitro motility of AtKCBP, a calmodulin-binding kinesin protein of *Arabidopsis*. Proc. Natl. Acad. Sci. USA *94*, 322–327.

Walker, R.A., O'Brien, E.T., Epstein, D.L., and Sheetz, M.P. (1997). n-Ethylmaleimide and ethacrynic acid inhibit kinesin binding to microtubules in a motility assay. Cell Motil. Cytoskeleton *37*, 289–299.

Walker, R.A., Salmon, E.D., and Endow, S.A. (1990). The *Drosophila claret* segregation protein is a minus-end directed motor molecule. Nature *347*, 780–782.

Wiese, C., and Zheng, Y. (1999). γ-Tubulin complexes and their interaction with microtubule-organizing centers. Curr. Opin. Struct. Biol. *9*, 250–259.

Zeng, X., Kahana, J.A., Silver, P.A., Morphew, M.K., McIntosh, J.R., Fitch, I.T., Carbon, J., and Saunders, W.S. (1999). Slk19p is a centromere protein that functions to stabilize mitotic spindles. J. Cell Biol. *146*, 415–425.